THE JOURNAL OF BIOLOGICAL CHEMISTRY VOL. 284, NO. 37, pp. 25160–25169, September 11, 2009

NDRG4 Is Required for Cell Cycle Progression and Survival in Glioblastoma Cells*[S]

Received for publication, April 23, 2009, and in revised form, July 9, 2009 Published, JBC Papers in Press, July 10, 2009, DOI 10.1074/jbc.M109.012484

Stephen H. Schilling[‡§1], Anita B. Hjelmeland[¶‖2], Daniel R. Radiloff[‡§], Irwin M. Liu[‡], Timothy P. Wakeman[‡], Jeffrey R. Fielhauer[**], Erika H. Foster[**], Justin D. Lathia[¶‖2], Jeremy N. Rich[‡¶‖‡‡§§2], Xiao-Fan Wang[‡§3], and Michael B. Datto[4]**

From the Departments of [‡]Pharmacology and Cancer Biology, [¶]Surgery, [**]Pathology, [‡‡]Medicine, and [§§]Neurobiology, the [§]Integrated Toxicology and Environmental Health Program, and the [‖]Preston Robert Tisch Brain Tumor Center, Duke University Medical Center, Durham, North Carolina 27710

NDRG4 is a largely unstudied member of the predominantly tumor suppressive N-Myc downstream-regulated gene (NDRG) family. Unlike its family members NDRG1–3, which are ubiquitously expressed, NDRG4 is expressed almost exclusively in the heart and brain. Given this tissue-specific expression pattern and the established tumor suppressive roles of the NDRG family in regulating cellular proliferation, we investigated the cellular and biochemical functions of NDRG4 in the context of astrocytes and glioblastoma multiforme (GBM) cells. We show that, in contrast to NDRG2, NDRG4 expression is elevated in GBM and NDRG4 is required for the viability of primary astrocytes, established GBM cell lines, and both $CD133^+$ (cancer stem cell (CSC)-enriched) and $CD133^-$ primary GBM xenograft cells. While NDRG4 overexpression has no effect on cell viability, NDRG4 knockdown causes G_1 cell cycle arrest followed by apoptosis. The initial G_1 arrest is associated with a decrease in cyclin D1 expression and an increase in $p27^{Kip1}$ expression, and the subsequent apoptosis is associated with a decrease in the expression of XIAP and survivin. As a result of these effects on cell cycle progression and survival, NDRG4 knockdown decreases the tumorigenic capacity of established GBM cell lines and GBM CSC-enriched cells that have been implanted intracranially into immunocompromised mice. Collectively, these data indicate that NDRG4 is required for cell cycle progression and survival, thereby diverging in function from its tumor suppressive family member NDRG2 in astrocytes and GBM cells.

The N-Myc downstream-regulated gene (NDRG)[5] family consists of four genes (NDRG1–4) that can be divided into two subfamilies based on sequence homology: NDRG1 and NDRG3 are in the first subfamily, and NDRG2 and NDRG4 make up the second subfamily. Although the four NDRG family members show distinct spatiotemporal expression patterns during embryonic development and in adult tissues (1–10), all four are highly expressed in the brain (4). To date, however, NDRG2 is the only NDRG family member that has been studied in the context of GBM cells and astrocytes. NDRG2 mRNA and protein levels are lower in GBM than in normal brain tissue, normal glial cells, and low grade astrocytomas (11–14), suggesting a tumor suppressive function. Data from experimental and clinical studies support this hypothesis: NDRG2 overexpression inhibits GBM cell proliferation (15), and decreased NDRG2 expression correlates with decreased GBM patient survival (13).

In contrast to its subfamily member NDRG2, NDRG4 has not been studied in GBM cells or astrocytes. Nevertheless, available evidence supports the hypothesis that NDRG4 has an important role in this context that is similar to the role of NDRG2. First, unlike the relatively ubiquitous expression patterns of NDRG1–3, NDRG4 expression is restricted to a small number of tissues including the brain, where it is expressed at particularly high levels (7, 10). This restricted expression pattern suggests that NDRG4 plays an important role within the central nervous system. Second, NDRG4 is more than 60% identical in amino acid sequence to NDRG2. This sequence similarity is likely behind the overlapping functions of these two proteins in certain cell types within the brain. For example, in PC12 neuronal cells, both NDRG4 and NDRG2 promote neurite extension (16–18). In combination with the brain-specific expression pattern of NDRG4, these functional and sequence similarities suggest that NDRG4 may recapitulate the tumor suppressive function of NDRG2 in primary brain neoplasms.

To determine if the similarities between NDRG2 and NDRG4 extend to the context of GBM, we investigated the role of NDRG4 in GBM cell lines and primary human astrocytes. In contrast to the established roles of NDRG2 and other NDRG family members, we found that the role of NDRG4 in GBM is not tumor suppressive. On the contrary, both astrocytes and GBM cells require the presence of NDRG4 for cell cycle progression and survival.

EXPERIMENTAL PROCEDURES

Plasmids—pLKO.1 lentiviral nontargeting shRNA clone, NDRG1 targeting shRNA clone (sh-NDRG1-a: NM_006096.2–779s1c1), and NDRG4 targeting shRNA clones (sh-NDRG4-a:

* This work was supported, in whole or in part, by National Institutes of Health Grant 1R01GM083000.

[S] The on-line version of this article (available at http://www.jbc.org) contains supplemental Figs. S1–S6.

[1] Supported by National Institutes of Health Grant T32ES07031 and an NSF Graduate Research Fellowship.

[2] Current affiliation: Dept. of Stem Cell Biology and Regenerative Medicine, Cleveland Clinic Foundation, Cleveland, OH 44195.

[3] To whom correspondence may be addressed: Duke University Medical Center, Dept. of Pharmacology and Cancer Biology, Box 3813, Durham, NC 27710. Tel.: 919-681-4861; Fax: 919-681-7152; E-mail: wang0011@mc.duke.edu.

[4] To whom correspondence may be addressed: Duke University Medical Center, Dept. of Pathology, Box 3712, Durham, NC 27710. Tel.: 919-684-6965; Fax: 919-684-6962; E-mail: michael.datto@duke.edu.

[5] The abbreviations used are: NDRG, N-Myc downstream-regulated gene; IHC, immunohistochemical; GBM, glioblastoma multiforme; CSC, cancer stem cell.

NM_020465.1–640s1c1; sh-NDRG4-b: NM_020465.1–769s1c1) were purchased from Sigma. pGIPZ lentiviral nontargeting shRNA clone and NDRG2 targeting shRNA clones (sh-NDRG2-a: RHS4430–99149037; sh-NDRG2-b: RHS4430–98851006) were purchased from Open Biosystems. pBabe-NDRG2 was generated by PCR amplification of NDRG2 from pCMV-HA-hNDRG2 (generously donated by Libo Yao and co-workers (15)) and subcloning into the BamHI and EcoRI sites of pBabe-puro. NDRG4 overexpression constructs were generated by PCR amplification of NDRG4(B) and NDRG4(H) from brain cDNA and subcloning into the BamHI site of pBabe-puro.

Generation of Overexpression and Knockdown Cells—Overexpression retrovirus was produced in 293T cells by co-transfection of pBabe constructs with the pCL10A-1 packaging vector. Knockdown lentivirus was produced in 293T cells by co-transfection with the psPAX2 and pVSVG packaging vectors. For both, medium was replenished 24 h after transfection, and virus was collected 48 h later. Supernatant was filtered, mixed with 4 μg/ml polybrene (Sigma), and added to target cells. For all experiments, cells were infected with virus for 48 h and selected with puromycin (1 μg/ml) for 72 h unless otherwise indicated.

Isolation of GBM CSCs and Nonstem Cells—Matched subpopulations of $CD133^+$ cells (enriched for GBM CSCs) and $CD133^-$ cells (nonstem cells) were isolated from human GBM xenografts or primary GBM tumors as previously described (19).

Cell Culture—GBM CSCs ($CD133^+$) were cultured in Neurobasal Medium without Phenol Red (Invitrogen) containing the following additives: B-27 supplement without vitamin A (Invitrogen), 20 ng/ml human recombinant epidermal growth factor (Invitrogen), 20 ng/ml human recombinant basic fibroblast growth factor (Invitrogen), GlutaMAX (Invitrogen), MEM nonessential amino acids solution (Invitrogen), and sodium pyruvate (Invitrogen). GBM nonstem cells ($CD133^-$) were cultured in Dulbecco's modified Eagle's medium supplemented with 10% fetal bovine serum. Normal primary human astrocytes were purchased from Lonza and cultured in the medium provided in the Astrocyte Medium BulletKit (CC-3186). All other GBM cell lines were cultured in Dulbecco's modified Eagle's medium supplemented with 10% fetal bovine serum.

Real-time Polymerase Chain Reaction—mRNA was isolated with the RNeasy Plus Mini Kit (Qiagen), and cDNA was synthesized using the SuperScript III First-Strand Synthesis System for RT-PCR (Invitrogen). Quantitative real-time PCR was performed using iQ SYBR Green Supermix (Bio-Rad), and results were normalized to β-2-microglobulin (B2M) levels. The following primers were used: NDRG4-F: GGAGGTTGTCTCTTTGGTCAAGGT, NDRG4-R: CTCATGACAGCAGCCACCAGAAT, B2M-F: GAGGTTTGAAGATGCCGCATT, B2M-R: TGTGGAGCAACCTGCTCAGATA.

Intracranial Tumor Formation Assay—Following infection and selection, 1,000 $CD133^+$ GBM CSCs or 300,000 U251 cells were implanted into the right frontal lobes of 5-week-old, male, athymic BALB/c nu/nu mice under a Duke University Institutional Animal Care and Use Committee-approved protocol. Mice were maintained for 6 months or until the development of neurological symptoms of functional impairment that significantly impaired their quality of life (ataxia, lethargy, seizures, and inability to feed). Because prior xenograft studies have demonstrated that these signs develop shortly before animal death, mice were euthanized at this point. Brains of euthanized mice were collected, fixed in 4% paraformaldehyde, paraffin-embedded, and sectioned. H&E staining and Ki-67 staining were performed by the Duke Pathology Research Histology Laboratory. The logrank test was used for statistical analysis.

Cell Viability (MTS), Annexin V, and Caspase 3/7 Activity Assays—Following infection and selection, the following numbers of cells per well were plated: 1,000 cells in 96-well plates (cell viability), 200,000 cells in 24-well plates (annexin V), and 5,000 cells in 96-well plates (caspase 3/7 activity). Assays were then carried out with the following kits: CellTiter® 96 AQ_{ueous} Nonradioactive Cell Proliferation Assay (Promega), Annexin V-PE Apoptosis Detection Kit (BD Biosciences), and Apo-ONE Homogenous Caspase-3/7 Assay (Promega).

Neurosphere Formation Assay—Following infection and selection, spheres of $CD133^+$ GBM CSCs were dissociated, and varying densities of cells were plated in 24-well plates. The percentage of wells with neurosphere formation and the average number of neurospheres per well were measured at the indicated times.

Flow Cytometry Cell Cycle Analysis—Prior to flow cytometry analysis, cells were fixed with 70% ethanol and then resuspended in 500 μl phosphate-buffered saline, 50 μl of PI (1 mg/ml), and 10 μl of RNase (20 mg/ml). For synchronization experiments, cells were first treated with 2 mM thymidine for 16 h. Cells were then washed, infected with knockdown lentivirus for 9 h, and treated with 2 mM thymidine again for 14 h before release. For spindle checkpoint experiments, cells were infected with knockdown lentivirus for 24 h and then treated for 48 h with 100 ng/ml nocodazole.

Western Analysis and Nucleocytoplasmic Fractionation—Nucleocytoplasmic fractionation was performed as described previously (20). For all other experiments, cells were lysed in ULB as described previously (21). Western analysis was performed using the following antibodies: phosphohistone H3-Ser-10 (Upstate, 06–570), γ-tubulin (Sigma, T6557), NDRG4 (Sigma, HPA015313), NDRG1 (Sigma, HPA006881), NDRG2 (Sigma, HPA002896), XIAP (Cell Signaling, 2045), caspase-3 (Cell Signaling, 9662), caspase-9 (Cell Signaling, 9508), cyclin D1 (Cell Signaling, 2926), cyclin E (Cell Signaling, 4129), Smad1 (Abcam, ab33902), α-tubulin (Abcam, ab6160), $p27^{Kip1}$ (Santa Cruz Biotechnology, sc-528), and lamin A/C (Santa Cruz Biotechnology, sc-7293).

Immunohistochemistry Analysis—Freshly frozen human glioma surgical resection samples from the Brain Tumor Center Tissue Bank at Duke University were processed, and 10 micron sections were mounted on glass slides in accordance with the Duke University Medical Center Institutional Review Board. Staining was then performed based on the protocol provided with R.T.U. VECTASTAIN Elite ABC Reagent (Vector Laboratories). Background Buster (Innovex Biosciences) was used for 30 min, NDRG4 antibody (1:25 dilution; Sigma, HPA015313) and biotinylated secondary antibody (10 μg/ml, Vector Laboratories) were used for 1 h each, and the Liquid DAB/Substrate

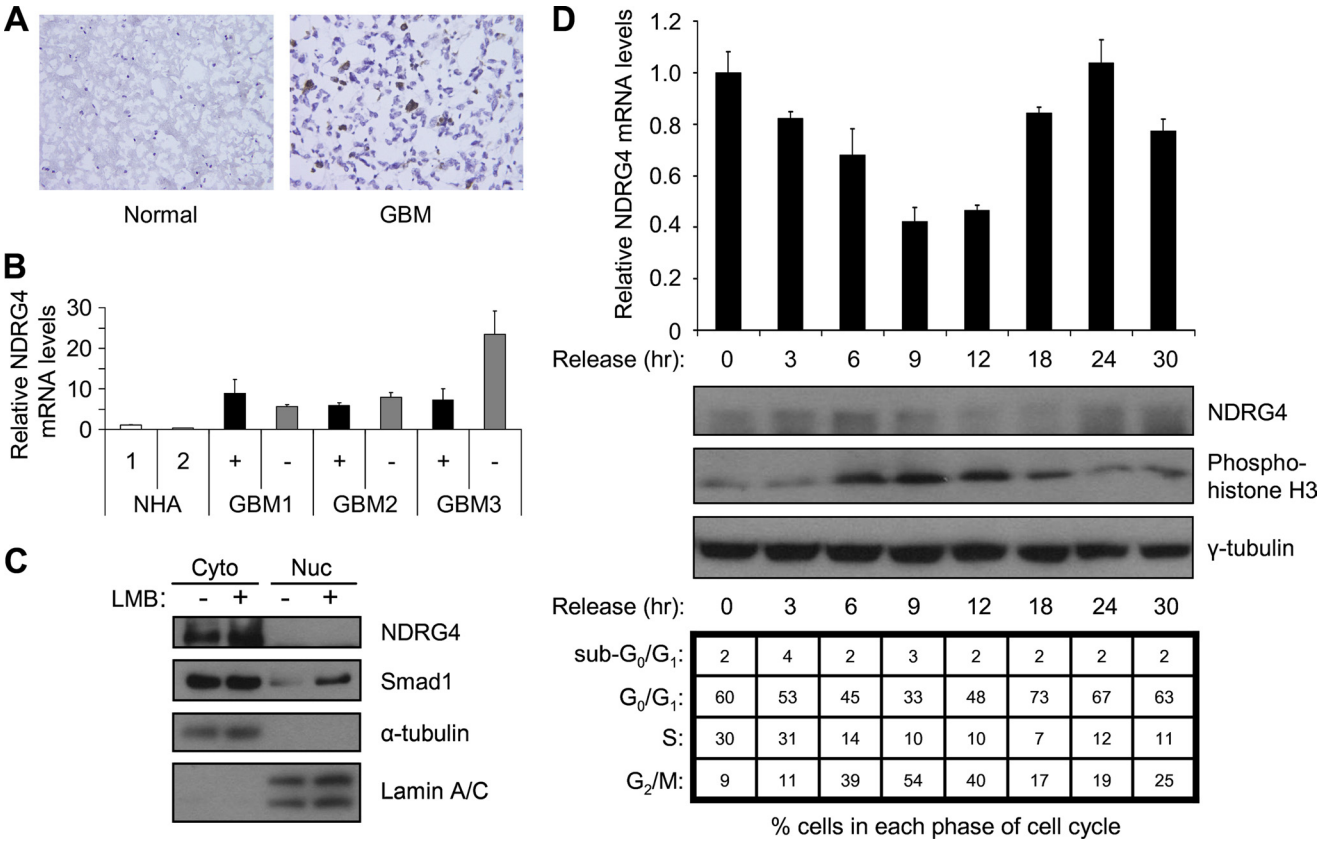

FIGURE 1. **Characterization of NDRG4 expression in GBM.** *A*, representative IHC images of NDRG4 expression in normal human cortex and GBM sections. *B*, real-time RT-PCR analysis of two independent lots of normal primary human astrocytes (*NHA 1* and *2*) and cultured cells derived from three human GBM xenograft samples (*GBM1*, 459 cells; *GBM2*, T4105 cells; *GBM3*, T3559 cells) and subsequently separated into GBM CSC-enriched (+) and nonstem cell (−) populations by CD133 status. *C*, nucleocytoplasmic fractionation of U251 cells and subsequent Western analysis. Smad1 served as a positive control for leptomycin B (*LMB*) treatment, and lamin A/C and α-tubulin were used as controls for nuclear (*nuc*) and cytoplasmic (*cyto*) fractions, respectively. *D*, real-time RT-PCR analysis and Western analysis of U251 cells partially synchronized with a double thymidine block and released for the indicated amounts of time. The percentage of cells in each phase of the cell cycle is indicated. γ-Tubulin was used as a loading control for Western analysis.

System (Innovex Biosciences) was used for 3 min. Ki-67 staining was performed by the Duke Pathology Research Histology Laboratory.

Single Cell Gel Electrophoresis (Comet Assay)—Cells were infected with knockdown or control lentivirus for 48 h, and comet assays were performed as described previously (22).

RESULTS

NDRG4 Expression Is Increased in GBM—To understand the role of NDRG4 in astrocytes and GBM cells and to determine the functional similarities and differences between NDRG4 and NDRG2, we began by studying NDRG4 expression in human tumor samples. Immunohistochemical (IHC) analysis of normal human cortex and GBM samples revealed increased NDRG4 protein expression in GBM (Fig. 1*A* and supplemental Fig. S1). Both normal samples tested had undetectable levels of NDRG4, but five out of six GBM samples showed a subset of neoplastic cells with moderate to high intensity cytoplasmic staining (supplemental Fig. S1). In the sample with the greatest degree of positivity, ~10–15% of cells showed strong staining for NDRG4 (Fig. 1*A*). This finding is in contrast to the reported lower expression level of NDRG2 in neoplastic glioma cells relative to normal nonneoplastic glial cells, an observation fitting with the presumed role of NDRG2 as a tumor suppressor in this context (11, 13, 14).

Our IHC analysis observations are further supported by an independent antibody-based proteomic analysis that showed increased NDRG4 expression in human glioma samples compared with nonneoplastic cortical brain tissue (11). Furthermore, a second NDRG4 antibody used in this independent IHC analysis of normal human tissues and cancer tissues yielded staining patterns similar to the those produced by the antibody used in Fig. 1*A* (11), suggesting that the staining pattern we observed is specifically due to increased NDRG4 expression. However, to confirm the increased expression of NDRG4 in GBM, we next examined NDRG4 mRNA levels in normal primary human astrocytes and cells derived from human GBM xenografts. Using primers specifically targeting an RNA sequence common to all known isoforms of NDRG4, we measured NDRG4 mRNA levels by real-time RT-PCR analysis in two independent lots of primary astrocytes and in cultured cells derived from three different GBM xenografts. Consistent with our IHC results, we found that NDRG4 expression was 5–20-fold higher in cultured GBM xenograft cells than in normal astrocytes (Fig. 1*B*).

Given that GBM tumors contain heterogeneous subpopulations of cells, we next tested whether the subset of cells showing strong NDRG4 staining represented the highly tumorigenic GBM CSC population. To test this, we examined the relative

expression level of NDRG4 in cultured GBM CSC-enriched populations ($CD133^+$) and corresponding nonstem cell populations ($CD133^-$) directly derived from GBM xenograft samples. The expression between these cell populations was similar (Fig. 1*B*). Thus, NDRG4 expression in GBM cells is not CSC-restricted.

NDRG4 Expression in GBM Is Cytoplasmic and Peaks during the G_1 and S Phases—Neoplastic GBM cells that were positive for NDRG4 expression by IHC analysis appeared to show strong cytoplasmic NDRG4 staining (Fig. 1*A* and supplemental Fig. S1), which is consistent with what has been reported in other cell types and in other species (2, 3). To confirm this localization in GBM cells and to further characterize the expression pattern of NDRG4, we determined its subcellular localization in U251 GBM cells by fractionation and Western analysis. Similar to what we observed through IHC analysis, NDRG4 localized to the cytoplasmic fraction (Fig. 1*C*). Furthermore, it remained cytoplasmic even upon treatment with the nuclear export inhibitor leptomycin B.

To begin to understand the biological functions of NDRG4, we next partially synchronized U251 cells with a double thymidine block and measured NDRG4 expression during different stages of the cell cycle. We found that NDRG4 levels fluctuate during cell cycle progression. At 9–12 h after release from the block, when the highest percentage of G_2/M cells was observed (~50%), NDRG4 mRNA levels were lowest (Fig. 1*D*). In contrast, NDRG4 mRNA levels peaked at 0–3 h and 18–24 h after release, and NDRG4 protein expression peaked slightly later in an expression pattern opposing that of the mitotic marker phosphohistone H3. These time points correlate with progression through G_1 phase and entry and progression through S phase. This is supported by our IHC analysis, which showed that similar percentages of GBM cells stain positive for NDRG4 and the proliferation marker Ki-67 (~10–15% and 15–20%, respectively; Fig. 1*A*, supplemental Fig. S1, and supplemental Fig. S2). It is also consistent with our observation that NDRG4 mRNA levels decrease with passage number in primary human astrocytes as they stop growing: NDRG4 expression levels at passage 7 were only 20% of what they were at passage 1 (supplemental Fig. S3), presumably due to a decreased percentage of astrocytes progressing through the G_1/S transition. A similar decrease in NDRG2 expression was observed with increasing passage. Taken together, these results prompted the additional comparative studies of NDRG2 and NDRG4 described below and indicated that NDRG4 is expressed in a cell cycle-specific manner that implicates it in cell cycle progression.

NDRG4 Is Required for GBM Cell Viability—To test the hypothesis that NDRG4 is involved in GBM cell cycle progression, we knocked down NDRG4 expression with two lentiviral shRNA constructs (sh-NDRG4-a and sh-NDRG4-b) that target different regions of the NDRG4 transcript, and we then assessed cell viability by MTS assay in the resulting knockdown cell lines. Knockdown of NDRG4 expression in U251 GBM cells dramatically decreased their viability (Fig. 2*A*). The magnitude of the reduction in viability was proportional to the efficacy of the two shRNA constructs: sh-NDRG4-a reduced NDRG4 expression and cell viability by ~60%, whereas sh-NDRG4-b reduced each by ~95%.

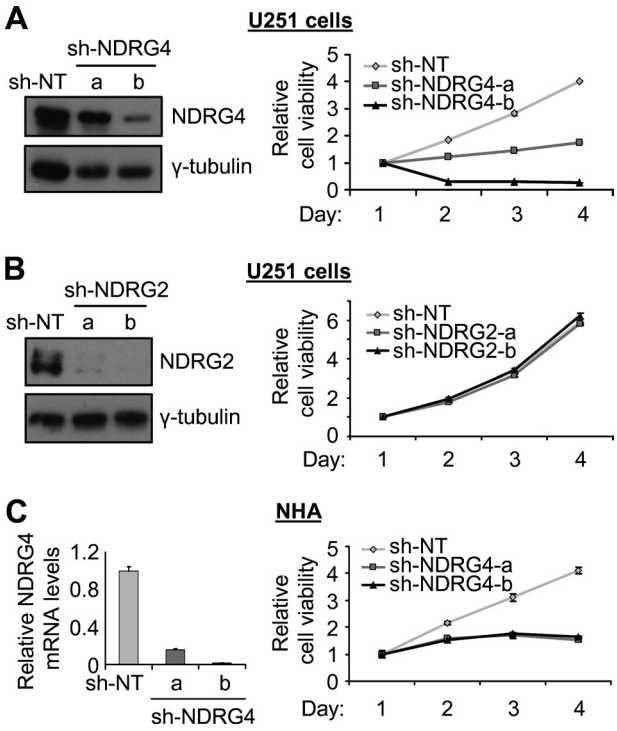

FIGURE 2. **Knockdown of NDRG4, but not NDRG2, decreases cell viability in normal primary human astrocytes and GBM cells.** *A*, Western analysis and MTS cell viability analysis of U251 control (*sh-NT*) and NDRG4 knockdown (*sh-NDRG4-a*, *sh-NDRG4-b*) cell lines. γ-Tubulin was used as a loading control for Western analysis. *B*, Western analysis and MTS cell viability analysis of U251 control (*sh-NT*) and NDRG2 knockdown (*sh-NDRG2-a*, *sh-NDRG2-b*) cell lines. *C*, real-time RT-PCR analysis and MTS cell viability analysis of control and NDRG4 knockdown normal primary human astrocytes (*NHA*). NDRG4 knockdown was confirmed by RT-PCR instead of Western analysis due to limited cell numbers.

These dose-dependent effects strongly suggest that the decreased viability we observed was a specific effect caused by loss of NDRG4 expression. This is further supported by our finding that cell viability was unaffected by control, nontargeting shRNAs (Fig. 2*A*). Similarly, shRNAs that target NDRG2 did not affect cell viability despite reducing NDRG2 protein levels by more than 90% (Fig. 2*B*). Moreover, NDRG1 and NDRG2 levels were not affected by NDRG4 knockdown (supplemental Fig. S4), further indicating that the effects on cell viability were specifically due to NDRG4 knockdown.

To determine if the decreased cell viability caused by NDRG4 knockdown is a robust response, we next knocked down NDRG4 expression in several additional GBM cell lines as well as primary astrocytes, the presumed cell of origination for GBM. In every GBM cell line tested, NDRG4 knockdown reduced cell viability by 40–99% (supplemental Fig. S5). Moreover, the NDRG4 knockdown-induced decrease in viability was not restricted to transformed or neoplastic cells, as 90–95% knockdown of NDRG4 decreased the viability of primary astrocytes by 60% (Fig. 2*C*). Thus, the reduction in cell viability caused by NDRG4 knockdown is a robust response that is not unique to the U251 cell line model system.

This robust requirement for the presence of NDRG4 is in contrast to the function of NDRG2 in GBM cells. While NDRG4 expression is essential for U251 cell viability (Fig. 2*A*), reduction of NDRG2 expression by ~95% did not affect the

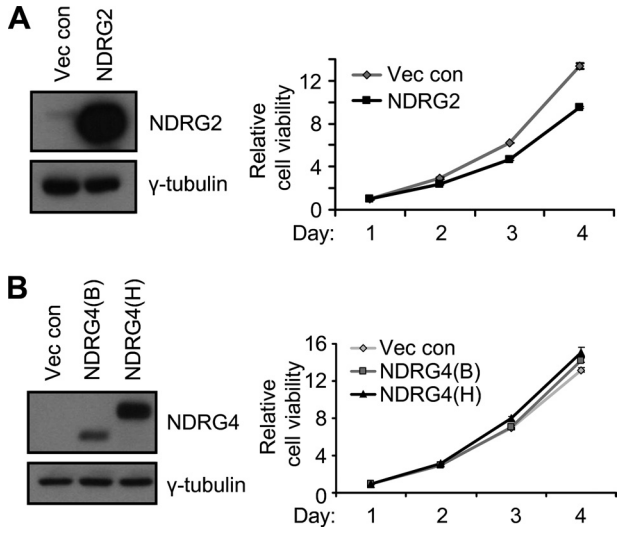

FIGURE 3. **Overexpression of NDRG2, but not NDRG4, decreases U251 cell viability.** *A*, Western analysis and MTS cell viability analysis of U251 control (*Vec con*) and NDRG2 overexpression cells. γ-Tubulin was used as a loading control for Western analysis. *B*, Western analysis and MTS cell viability analysis of U251 control (*Vec con*) and NDRG4 overexpression cells. Two isoforms of NDRG4 were overexpressed: the B isoform (*NDRG4(B)*) and the H isoform (*NDRG4(H)*). γ-Tubulin was used as a loading control for Western analysis.

viability of U251 cells (Fig. 2*B*). Severalfold overexpression of NDRG2, however, reduced U251 cell viability by 30% at day 4 (Fig. 3*A*), which is consistent with previous findings from NDRG2 overexpression studies in U373 GBM cells (15). In contrast, severalfold overexpression of two NDRG4 isoforms that have been demonstrated to be expressed in the brain, NDRG4(B) and NDRG4(H), did not affect U251 cell viability (Fig. 3*B*). Thus, despite the strong similarity between NDRG2 and NDRG4 in sequence and in function in other cell types, our results indicate that these two genes have divergent functions in GBM cells.

Loss of NDRG4 in GBM Cells Results in G_1 Cell Cycle Arrest and Subsequent Apoptosis—Loss of cell viability as determined by MTS assay can have multiple etiologies including reduced metabolic activity, cell cycle arrest, and apoptosis. To differentiate between the possible etiologies, we knocked down NDRG4 expression in U251 cells that had been partially synchronized in early S phase by a double thymidine block, and we then measured the percentage of cells in each phase of the cell cycle after release. While control cells completed two cell cycles in a 36 h time window, cells with reduced NDRG4 expression completed the first cycle but stopped cycling in the G_1 phase of the second cycle (Fig. 4*A*). This indicated that NDRG4 is required for progression through G_1. To further confirm this, we did cell cycle analysis over an NDRG4 knockdown time course. A comparison of U251 cells at day 1 and day 1.5 after infection with sh-NDRG4-b knockdown virus revealed an increase in the percentage of cells in G_1 at day 1.5 (from 69 to 84%) and a corresponding decrease in the percentage of cells in S and G_2/M (from 30 to 15%; Fig. 4*B*). Moreover, we detected a number of NDRG4 knockdown-induced molecular events associated with the regulation of G_1 phase progression: $p27^{Kip1}$ levels increased and cyclin D1 levels decreased starting at day 1 after infection with the sh-NDRG4-b knockdown virus (Fig. 4*C*).

NDRG4 knockdown-induced G_1 arrest was followed by several apoptotic events. The initial accumulation of cells in G_1 that was first observed at day 1.5 after infection with sh-NDRG4-b knockdown virus was followed by a slight decrease in the G_1 population of cells at day 4 (92% at day 3.5 and 85% at day 4; Fig. 4*B*). This corresponded with an increase in the sub-G_0/G_1 population (2% at day 3.5 and 9% at day 4), which is suggestive of increased apoptosis. In support of this, NDRG4 knockdown caused a 5-fold increase over control in the percentage of annexin V-positive cells at day 5 (Fig. 4*D*). Furthermore, a number of molecular events associated with apoptosis were observed in NDRG4 knockdown cells but not control cells: XIAP and survivin levels decreased starting at day 2 after infection with sh-NDRG4-b virus, and this was followed by an increase in caspase cleavage at day 3 (Fig. 4*E*). The elevation in caspase activity was confirmed by fluorescent caspase 3/7 activity assays, which revealed an 11-fold increase in caspase activity in response to knockdown with the sh-NDRG4-b virus (Fig. 4*F*). The sh-NDRG4-a construct produced similar, although attenuated, effects consistent with its less pronounced effect on NDRG4 expression.

Loss of NDRG4 Does Not Induce DNA Damage or Affect Mitotic Progression—During the G_1 phase of the cell cycle, safeguards exist to ensure that genomic DNA is intact and ready for replication. Consequently, progression through G_1 can be stopped by factors that cause a loss of genomic DNA integrity due to improper mitosis. Because another NDRG family member, NDRG1, is required for correct mitotic spindle formation and progression through mitosis in mammary epithelial cells (23), we next used a mitotic checkpoint assay to investigate whether NDRG4 functions in an analogous manner in GBM cells. Treatment of control cells with nocodazole, a chemotherapeutic inhibitor of microtubule formation that interferes with the formation of the mitotic spindle, resulted in an increased polyploid population of cells manifesting as 4N and 8N cells (46 and 16% of cells, respectively, as compared with 10 and 1% of untreated cells; Fig. 5*B*). The presence of polyploidy rather than mitotic arrest is likely due to the mutated TP53 gene present in U251 cells. As expected, NDRG1 knockdown exacerbated the detrimental effect of nocodazole. The combined result of nocodazole treatment and a loss of NDRG1 was a dramatic increase in apoptosis manifesting as a large sub-G_0/G_1 population of cells (31% of cells as compared with 12% in the control nocodazole-treated population; Fig. 5, *A* and *B*). In contrast, NDRG4 knockdown in combination with nocodazole treatment did not cause pronounced apoptosis or polyploidy, but rather led to the accumulation of 2N and 4N cells (50 and 32% of cells, respectively, as compared with 10 and 46% in the control nocodazole-treated population), presumably due to an inability of the cells to enter S phase (Fig. 5, *A* and *B*). The differing effects of NDRG1 and NDRG4 knockdown in this context suggest that NDRG1 and NDRG4 have different biological functions and that the G_1 block and subsequent apoptosis caused by NDRG4 knockdown are not due to chromosomal defects acquired during mitosis.

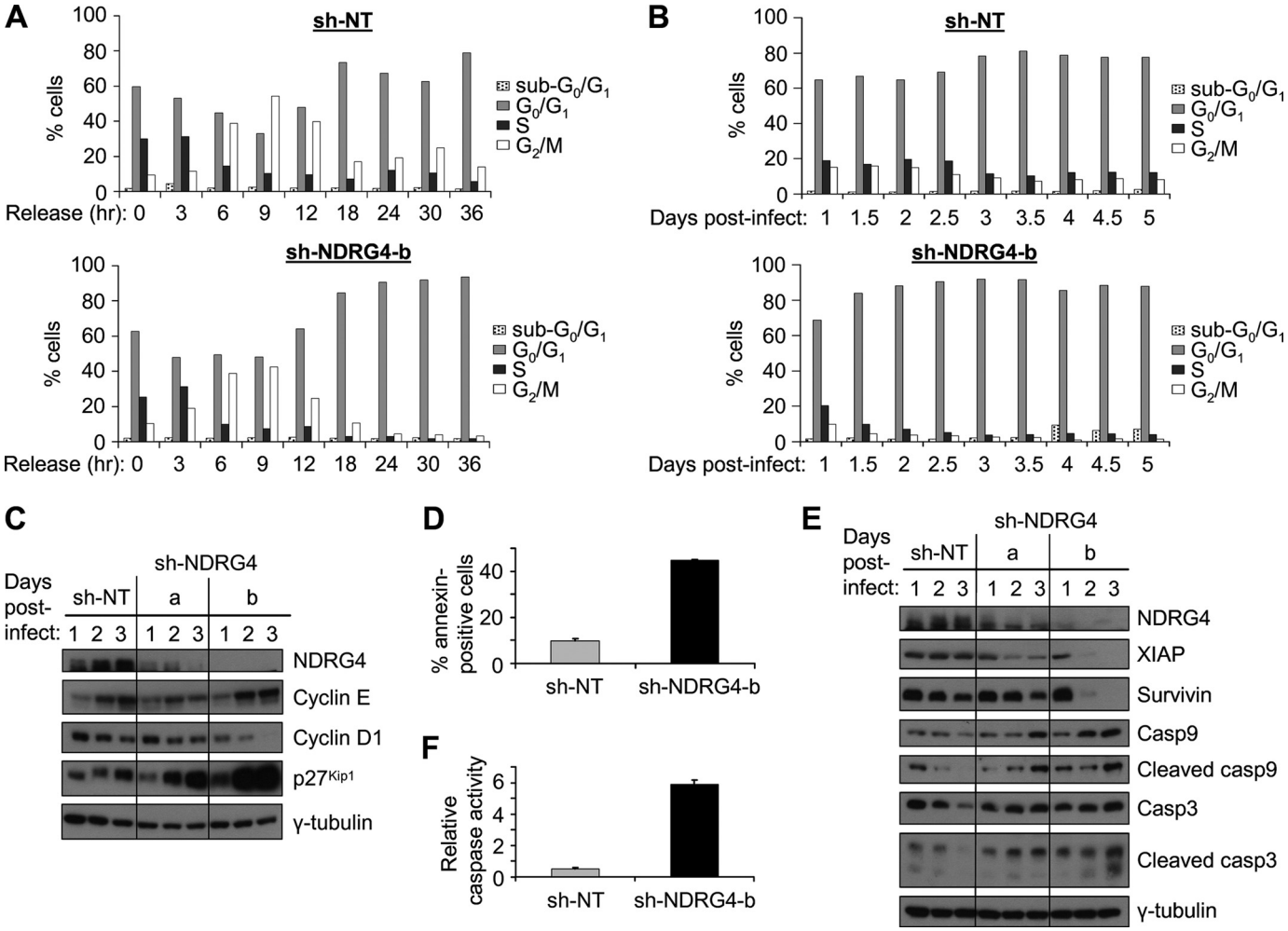

FIGURE 4. **NDRG4 knockdown causes G_1 arrest and subsequent apoptosis in U251 cells.** *A*, cell cycle analysis following partial synchronization with a double thymidine block. Control (*sh-NT*) and NDRG4 knockdown (*sh-NDRG4-b*) cells were analyzed at the indicated time points following release from block. *B*, cell cycle analysis following infection with control virus (*sh-NT*) or NDRG4 knockdown virus (*sh-NDRG4-b*) for the indicated number of days. *C*, Western analysis of G_1 cell cycle progression markers in control cells (*sh-NT*) and NDRG4 knockdown cells (*sh-NDRG4-a*, *sh-NDRG4-b*) following infection with control virus or NDRG4 knockdown virus for 1 day, 2 days, and 3 days. γ-Tubulin was used as a loading control. *D*, percentage of annexin V-positive cells in NDRG4 knockdown (*sh-NDRG4-b*) and control (*sh-NT*) cell populations at day 5 after infection. *E*, Western analysis of apoptotic markers in control cells (*sh-NT*) and NDRG4 knockdown cells (*sh-NDRG4-a*, *sh-NDRG4-b*) following infection with control virus or NDRG4 knockdown virus for 1 day, 2 days, and 3 days. γ-Tubulin was used as a loading control. *F*, caspase-3/7 activity, as determined by colorimetric assay, in knockdown (*sh-NDRG4-b*) and control (*sh-NT*) cell populations at day 5 after infection.

Another common cause of G_1 arrest is DNA damage. However, DNA damage is also unlikely to be the cause of the NDRG4 knockdown-induced G_1 arrest. While DNA double-strand break-inducing ionizing radiation caused formation of "comet tails" characteristic of DNA damage in U251 cells (Fig. 5*C*), NDRG4 knockdown did not induce any noticeable "comet tail" formation in these comet assays (Fig. 5*C*). These results, in combination with the exclusive cytoplasmic localization of NDRG4, strongly suggest that DNA damage and mitotic defects are not the cause of G_1 arrest and apoptosis in NDRG4 knockdown cells.

NDRG4 Is Required for the Viability and Self-renewal of GBM CSC-enriched CD133$^+$ Cells and Nonstem Cell-enriched CD133$^-$ Cells—GBM tumors are heterogeneous populations of cells that include GBM CSCs, which are characterized by the ability to self-renew and recapitulate their parental tumors in immunocompromised mice (24–26). To determine if NDRG4 behaves differently in GBM CSC-enriched populations (CD133$^+$) and corresponding nonstem cell-enriched populations (CD133$^-$), we isolated these subpopulations of cells from human GBM xenografts derived from primary GBMs. The GBM CSC-enriched cell lines were previously validated by the expression of stem cell markers and were characterized as capable of differentiating into multiple brain cell lineages and potently forming tumors that recapitulate the heterogeneity of their parental tumors (19, 27). Using these GBM CSC-enriched cells and corresponding nonstem cell-enriched cells, we found that the role of NDRG4 in cell cycle progression and cell viability in both populations is the same as in the immortalized GBM cell line model systems.

In GBM CSC-enriched cells, NDRG4 knockdown decreased viability in a dose-dependent manner. Consistent with the level of knockdown produced by each, sh-NDRG4-a decreased cell viability by 60% at day 4 and sh-NDRG4-b decreased cell viability by 80% (Fig. 6*A*). Similar results were seen with the neurosphere formation assay (Fig. 6, *B* and *C*). When equivalent num-

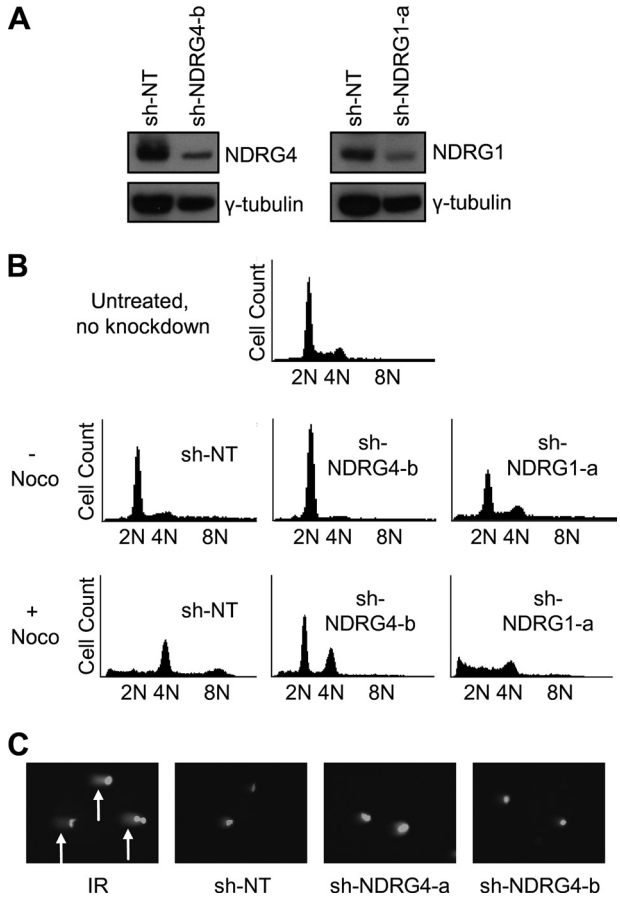

FIGURE 5. **NDRG4 knockdown-induced cell cycle arrest and apoptosis in U251 cells are not due to mitotic defects or DNA damage.** *A*, Western analysis of control (*sh-NT*), NDRG4 knockdown (*sh-NDRG4-b*), and NDRG1 knockdown (*sh-NDRG1-a*) cells. γ-Tubulin was used as a loading control. *B*, flow cytometry analysis of cells that were first infected with control, NDRG1, or NDRG4 knockdown virus for 24 h and then treated with nocodazole (+*Noco*) or left untreated (−*Noco*) for 48 h. DNA content (*2N*, *4N*, and *8N*) is represented on the *x* axis. *C*, comet assays in control (*sh-NT*) and NDRG4 knockdown (*sh-NDRG4-a*, *sh-NDRG4-b*) cells. Cells exposed to 10 Gy of ionizing radiation (*IR*) were used as a positive control for DNA damage-induced "comet tails" (indicated by *arrows*).

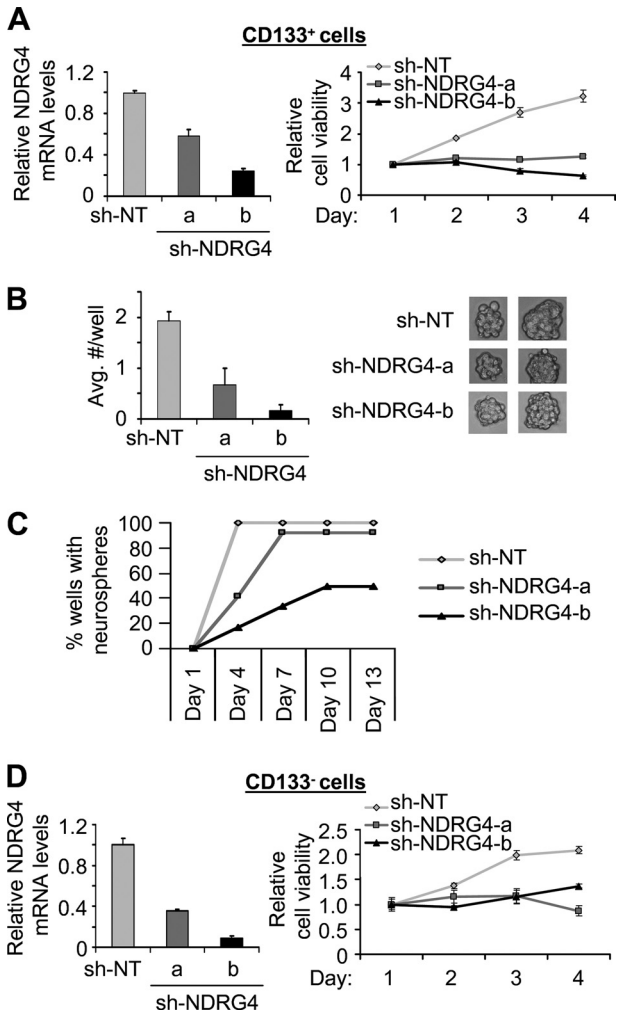

FIGURE 6. **Knockdown of NDRG4 decreases viability and self-renewal of both CD133$^+$ and CD133$^-$ GBM cells.** *A*, real-time RT-PCR analysis and MTS cell viability analysis of control (*sh-NT*) and NDRG4 knockdown (*sh-NDRG4-a*, *sh-NDRG4-b*) GBM CSC-enriched CD133$^+$ cells isolated from a T4105 human GBM xenograft. Knockdown was confirmed by RT-PCR instead of Western analysis due to limited cell numbers. *B*, average number of neurospheres formed per well at day 4 of neurosphere formation assay. CD133$^+$ cells were initially plated out at a density of 100 cells per well. Representative images of neurospheres are shown. *C*, percentage of wells containing neurospheres over time. CD133$^+$ cells were initially plated out at densities of 100 cells per well. *D*, real-time RT-PCR analysis and MTS cell viability analysis of control and NDRG4 knockdown CD133$^-$ GBM cells isolated from a T4302 human GBM xenograft. Knockdown was confirmed by RT-PCR instead of Western analysis because of limited cell numbers.

bers of cells were plated, the number of neurospheres formed per well decreased with NDRG4 targeting (65% decrease with sh-NDRG4-a and 90% decrease with sh-NDRG4-b at day 4 after plating cells; Fig. 6*B*). Depending on the extent of NDRG4 knockdown, there was also a delay in the time necessary to form neurospheres or a decrease in the percentage of wells with neurosphere formation (Fig. 6*C*).

Just as NDRG4 knockdown decreased the viability of CSC-enriched CD133$^+$ GBM cells, it also decreased the viability of nonstem cell-enriched CD133$^-$ GBM cells. A 40–60% decrease in viability was observed at day 4 with both NDRG4 knockdown constructs, which reduced NDRG4 expression by 65 and 90% (Fig. 6*D*). Together, these data indicate that NDRG4 is required for the survival and self-renewal potential of both GBM CSC-enriched populations and GBM nonstem cell populations.

Knockdown of NDRG4 Decreases Growth of GBM Tumor Xenografts in Immunocompromised Mice—To confirm that NDRG4 does indeed behave differently than NDRG2 in the context of GBM, we assessed whether the decreased viability resulting from NDRG4 knockdown in cell culture translates into similar effects on GBM cells *in vivo*. To address this, we used a mouse tumor model system that best approximates the microenvironment of a GBM tumor. Prior to NDRG4 knockdown-induced apoptosis, we implanted U251 control and NDRG4 knockdown cells intracranially into immunocompromised mice. Consistent with our cell culture data, there was a statistically significant decrease and delay in the development of functional impairment caused by brain tumor formation in mice injected with either population of NDRG4 knockdown cells compared with the mice injected with control cells ($p <$ .001 for both sh-NDRG4-a and -b; Fig. 7*A*).

Comparable results were seen with GBM CSC-enriched cells. As with the U251 cells, control and NDRG4 knockdown

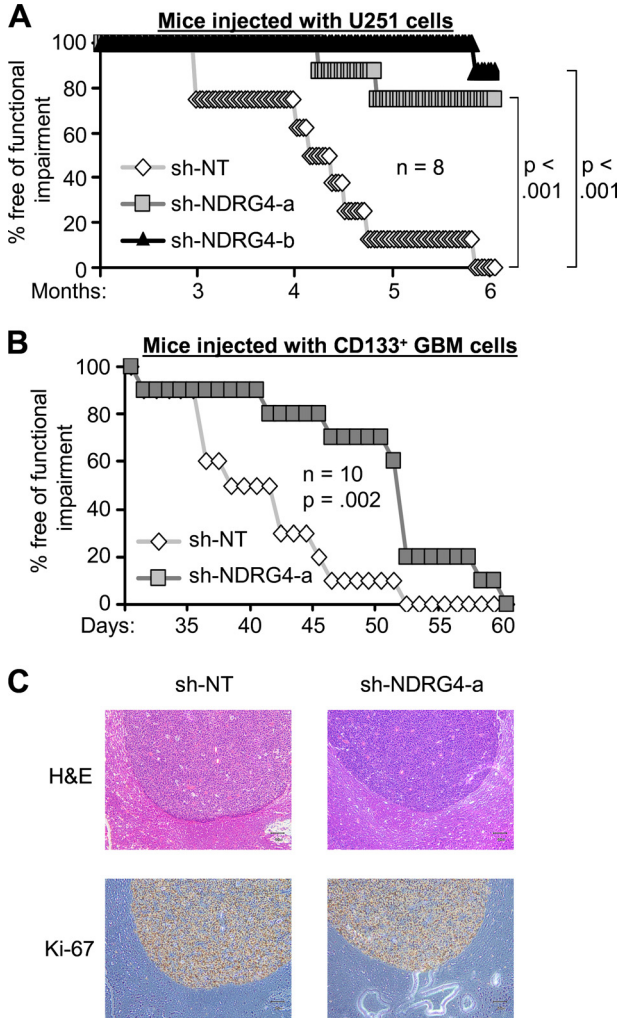

FIGURE 7. **Knockdown of NDRG4 decreases growth of GBM tumor xenografts in immunocompromised mice.** *A*, percentage of mice that remained free of neurological functional impairment over time after being injected intracranially with U251 control cells (*sh-NT*) or NDRG4 knockdown cells (*sh-NDRG4-a*, *sh-NDRG4-b*). Neurological functional impairment included ataxia, lethargy, seizures, and inability to feed. *B*, percentage of mice that remained free of neurological functional impairment over time after being injected intracranially with control (*sh-NT*) or NDRG4 knockdown (*sh-NDRG4-a*) $CD133^+$ GBM CSC-enriched cells. $CD133^+$ cells were originally isolated from a T3559 human GBM xenograft. *C*, representative H&E and Ki-67 staining images of brain sections from mice injected with control and NDRG4 knockdown $CD133^+$ cells.

GBM CSC-enriched cells were implanted intracranially into immunocompromised mice. We found a statistically significant delay in the development of functional impairment caused by tumor formation in the mice injected with sh-NDRG4-a knockdown cells compared with the mice injected with control cells ($p = .002$, Fig. 7*B*). Tumor formation was confirmed by H&E staining and Ki-67 staining of brains resected from sacrificed mice. Representative images are shown in Fig. 7*C*. Collectively, these data reveal that NDRG4 is required for the viability of GBM cell lines *in vitro* and *in vivo*. Thus, NDRG4 diverges in function from its family member NDRG2 and does not act as a tumor suppressor in GBM.

DISCUSSION

Here we report the first characterization of NDRG4 in G_1 cell cycle progression and survival and the first characterization of NDRG4 function in the context of astrocytes and GBM cells. We show that the function of NDRG4 diverges from the function of NDRG2 in GBM cells: NDRG2 overexpression decreases GBM cell viability, whereas NDRG4 is required for G_1 progression and cell viability in a number of different GBM and astrocyte model systems. This is the first direct comparison and characterization of the diverse and divergent cellular functions of the NDRG family.

NDRG4 Is Required for Cell Cycle Progression and the Survival of GBM Cells—NDRG4 expression fluctuates throughout the cell cycle, with maximal expression occurring during the G_1 and S phases. Loss of NDRG4 through targeted knockdown leads to cell cycle arrest in G_1 with an associated increase in $p27^{Kip1}$ levels and a decrease in cyclin D1 but not cyclin E levels. Taken together, these findings suggest that NDRG4 plays a critical role in the transition between the G_1 and S phases of the cell cycle.

Because cyclin D-CDK complexes are important for progression through early G_1 and cyclin E-CDK complexes are important for progression through late G_1 (28), G_1 arrest caused by NDRG4 knockdown likely occurs in early G_1 phase due to reduced cyclin D1 levels. However, increased $p27^{Kip1}$ expression has been demonstrated to prevent activation of cyclin E-CDK2 complexes (29), so NDRG4 knockdown likely also affects progression through late G_1. Although the precise molecular function of NDRG4 at the G_1 to S transition remains to be determined, we detected no DNA damage or defects in mitosis following NDRG4 knockdown, so it is unlikely that DNA damage or chromosome disruption is causing NDRG4 knockdown-induced cell cycle arrest. Furthermore, loss of NDGR4 likely has broader effects than simply preventing the start of S phase through CDKI activation or the regulation of critical cell cycle proteins, as NDRG4 knockdown cells ultimately undergo apoptosis.

The apoptosis caused by NDRG4 knockdown is associated with a decrease in the levels of both XIAP and survivin. XIAP and survivin are required for glioma growth and tumor formation (30–32), and high expression of these proteins is associated with poor prognosis in GBM patients (33–35). Because of the importance of these antiapoptotic proteins, inhibitors or knockdown reagents targeting XIAP can directly induce apoptosis in GBM cell lines and can act synergistically with other chemical inducers of apoptosis to cause death in cells with significant intrinsic resistance to toxic agents (30, 32, 36, 37). Given the critical role of these proteins in glioma cell survival, the loss of XIAP and survivin protein expression in NDRG4 knockdown cells may underlie the observed apoptotic effects.

The Role of NDRG4 in GBM Diverges from Previously Characterized Functions of the NDRG Family—Although our findings are consistent with recent findings in zebrafish embryos, where NDRG4 expression corresponds with proliferative stages of heart development and NDRG4 function is important for myocyte proliferation (6), the requirement of NDRG4 for the viability of GBM tumor cells and astrocytes differs from the pro-differentiation and growth inhibitory roles of NDRG4 in neurons and pancreatic cells. In nerve growth factor (NGF)-treated PC12 neuronal cells, NDRG4 knockdown reduces AP-1 activation and inhibits neurite extension (17). Overexpression

of NDRG4 in the same cells enhances NGF-induced phosphorylation of MEK and ERK, presumably also enhancing differentiation (16). Similarly, NDRG4 expression is required for glucagon-like-polypeptide-1-induced growth inhibition and endocrine differentiation in rat pancreatic cells (38).

The role of NDRG4 in GBM also differs from the function of NDRG2 in the same context. Within the NDRG family, NDRG4 is most similar to NDRG2, with ~65% identity at the amino acid sequence level (10). Accordingly, these two NDRG family members have similar functions in some cell types within the brain. In GBM cells, however, the opposite is true. Although the mRNA expression levels of NDRG2 and NDRG4 are weakly positively correlated in GBM samples (supplemental Fig. S6) (39), NDRG2 and NDRG4 have opposing protein expression patterns when comparing normal brain tissue to GBM tissue, and NDRG4 appears to have a function that diverges significantly from NDRG2. While overexpression of NDRG2 reduces GBM cell viability, knockdown of NDRG2 expression in the same cells has no effect. In contrast, overexpression of NDRG4(B) and NDRG4(H) does not affect GBM cell viability, while NDRG4 knockdown decreases the viability of the same cells.

When these opposing functions of NDRG4 and NDRG2 in GBM are taken in the context of the NDRG family in general, it is the function of NDRG2 that is consistent with the prevailing theories regarding the roles of these genes as tumor suppressors. Just as NDRG2 expression levels are reduced in GBM, decreased NDRG2 expression is observed in colorectal adenocarcinoma (40, 41), and thyroid (42), hepatocellular (43), gastric (44), and clear cell renal (45) carcinomas. Consistent with these expression patterns, NDRG2 has been reported to suppress cellular proliferation (44, 46), suppress invasion and metastasis (43), and be required for apoptotic pathways including Fas-mediated cell death (44) and p53-mediated apoptosis (47). The expression patterns and functions of NDRG1 in cancer mostly mirror those of NDRG2. NDRG1 expression is reduced in many cancer types (48–52), and NDRG1 can inhibit cellular proliferation (53) and tumor metastasis (49) and is an effector for both p53-mediated apoptosis (54) and the tumor suppressive effects of PTEN (55). NDRG3 has not been studied as extensively, but recent findings in prostate cancer suggest that it may behave differently than NDRG1 and NDRG2, as it promotes cell growth in this context (56). Taken together, however, the available evidence indicates that a major function of NDRG family members is to impede cancer progression through the regulation of proliferation, apoptosis, and metastasis (57, 58). Thus, our discovery that NDRG4 is required for the viability of GBM cells and astrocytes challenges the view that NDRG family members are fundamentally tumor suppressive.

In summary, our study establishes a novel role for NDRG4 that is in contrast to the known functions of NDRG2 and its other family members. Specifically, we show that the presence of NDRG4 is required for the viability of GBM cell populations and primary astrocytes. In GBM cells, we demonstrate that the presence of NDRG4 is required for continued progression through the cell cycle and ultimately for survival. As we learn more about precisely how NDRG4 functions and how it is regulated in GBM cells and astrocytes, we will be able to further dissect apart the diverse and divergent functions of the NDRG family.

Acknowledgments—We thank the Duke University Flow Cytometry Facility for FACS assistance and Kenneth H. Young, Yong Yu, and Qiulian Wu for technical support.

REFERENCES

1. Kyuno, J., Fukui, A., Michiue, T., and Asashima, M. (2003) *Biochem. Biophys. Res. Commun.* **309,** 52–57
2. Nakada, N., Hongo, S., Ohki, T., Maeda, A., and Takeda, M. (2002) *Brain Res. Dev. Brain Res.* **135,** 45–53
3. Nishimoto, S., Tawara, J., Toyoda, H., Kitamura, K., and Komurasaki, T. (2003) *Eur. J. Biochem.* **270,** 2521–2531
4. Okuda, T., Kokame, K., and Miyata, T. (2008) *J. Histochem. Cytochem.* **56,** 175–182
5. Okuda, T., and Kondoh, H. (1999) *Biochem. Biophys. Res. Commun.* **266,** 208–215
6. Qu, X., Jia, H., Garrity, D. M., Tompkins, K., Batts, L., Appel, B., Zhong, T. P., and Baldwin, H. S. (2008) *Dev. Biol.* **317,** 486–496
7. Qu, X., Zhai, Y., Wei, H., Zhang, C., Xing, G., Yu, Y., and He, F. (2002) *Mol. Cell Biochem.* **229,** 35–44
8. Yamauchi, Y., Hongo, S., Ohashi, T., Shioda, S., Zhou, C., Nakai, Y., Nishinaka, N., Takahashi, R., Takeda, F., and Takeda, M. (1999) *Brain Res. Mol. Brain Res.* **68,** 149–158
9. Zhao, W., Tang, R., Huang, Y., Wang, W., Zhou, Z., Gu, S., Dai, J., Ying, K., Xie, Y., and Mao, Y. (2001) *Biochim. Biophys. Acta* **1519,** 134–138
10. Zhou, R. H., Kokame, K., Tsukamoto, Y., Yutani, C., Kato, H., and Miyata, T. (2001) *Genomics* **73,** 86–97
11. Berglund, L., Björling, E., Oksvold, P., Fagerberg, L., Asplund, A., Al-Khalili Szigyarto, C., Persson, A., Ottosson, J., Wernérus, H., Nilsson, P., Lundberg, E., Sivertsson, A., Navani, S., Wester, K., Kampf, C., Hober, S., Pontén, F., and Uhlén, M. (2008) *Mol. Cell Proteomics* **7,** 2019–2027
12. Felsberg, J., Yan, P. S., Huang, T. H., Milde, U., Schramm, J., Wiestler, O. D., Reifenberger, G., Pietsch, T., and Waha, A. (2006) *Neuropathol. Appl. Neurobiol.* **32,** 517–524
13. Madhavan, S., Zenklusen, J. C., Kotliarov, Y., Sahni, H., Fine, H. A., and Buetow, K. (2009) *Mol. Cancer Res.* **7,** 157–167
14. Tepel, M., Roerig, P., Wolter, M., Gutmann, D. H., Perry, A., Reifenberger, G., and Riemenschneider, M. J. (2008) *Int. J. Cancer* **123,** 2080–2086
15. Deng, Y., Yao, L., Chau, L., Ng, S. S., Peng, Y., Liu, X., Au, W. S., Wang, J., Li, F., Ji, S., Han, H., Nie, X., Li, Q., Kung, H. F., Leung, S. Y., and Lin, M. C. (2003) *Int. J. Cancer* **106,** 342–347
16. Hongo, S., Watanabe, T., Takahashi, K., and Miyazaki, A. (2006) *J. Cell. Biochem.* **98,** 185–193
17. Ohki, T., Hongo, S., Nakada, N., Maeda, A., and Takeda, M. (2002) *Brain Res. Dev. Brain Res.* **135,** 55–63
18. Takahashi, K., Yamada, M., Ohata, H., Honda, K., and Yamada, M. (2005) *Neurosci. Lett.* **388,** 157–162
19. Bao, S., Wu, Q., Sathornsumetee, S., Hao, Y., Li, Z., Hjelmeland, A. B., Shi, Q., McLendon, R. E., Bigner, D. D., and Rich, J. N. (2006) *Cancer Res.* **66,** 7843–7848
20. Jian, H., Shen, X., Liu, I., Semenov, M., He, X., and Wang, X. F. (2006) *Genes Dev.* **20,** 666–674
21. Waddell, D. S., Liberati, N. T., Guo, X., Frederick, J. P., and Wang, X. F. (2004) *J. Biol. Chem.* **279,** 29236–29246
22. Wakeman, T. P., Kim, W. J., Callens, S., Chiu, A., Brown, K. D., and Xu, B. (2004) *Mutat. Res.* **554,** 241–251
23. Kim, K. T., Ongusaha, P. P., Hong, Y. K., Kurdistani, S. K., Nakamura, M., Lu, K. P., and Lee, S. W. (2004) *J. Biol. Chem.* **279,** 38597–38602
24. Galli, R., Binda, E., Orfanelli, U., Cipelletti, B., Gritti, A., De Vitis, S., Fiocco, R., Foroni, C., Dimeco, F., and Vescovi, A. (2004) *Cancer Res.* **64,** 7011–7021
25. Singh, S. K., Clarke, I. D., Terasaki, M., Bonn, V. E., Hawkins, C., Squire, J., and Dirks, P. B. (2003) *Cancer Res.* **63,** 5821–5828

26. Singh, S. K., Hawkins, C., Clarke, I. D., Squire, J. A., Bayani, J., Hide, T., Henkelman, R. M., Cusimano, M. D., and Dirks, P. B. (2004) *Nature* **432,** 396–401
27. Bao, S., Wu, Q., McLendon, R. E., Hao, Y., Shi, Q., Hjelmeland, A. B., Dewhirst, M. W., Bigner, D. D., and Rich, J. N. (2006) *Nature* **444,** 756–760
28. Donjerkovic, D., and Scott, D. W. (2000) *Cell Res.* **10,** 1–16
29. Polyak, K., Kato, J. Y., Solomon, M. J., Sherr, C. J., Massague, J., Roberts, J. M., and Koff, A. (1994) *Genes Dev.* **8,** 9–22
30. Naumann, U., Bähr, O., Wolburg, H., Altenberend, S., Wick, W., Liston, P., Ashkenazi, A., and Weller, M. (2007) *Gene Ther.* **14,** 147–161
31. Zhen, H. N., Li, L. W., Zhang, W., Fei, Z., Shi, C. H., Yang, T. T., Bai, W. T., and Zhang, X. (2007) *Int. J. Oncol.* **31,** 1111–1117
32. Ziegler, D. S., Wright, R. D., Kesari, S., Lemieux, M. E., Tran, M. A., Jain, M., Zawel, L., and Kung, A. L. (2008) *J. Clin. Invest.* **118,** 3109–3122
33. Kogiku, M., Ohsawa, I., Matsumoto, K., Sugisaki, Y., Takahashi, H., Teramoto, A., and Ohta, S. (2008) *J. Clin. Neurosci.* **15,** 1198–1203
34. Schimmer, A. D., Dalili, S., Batey, R. A., and Riedl, S. J. (2006) *Cell Death Differ* **13,** 179–188
35. Uematsu, M., Ohsawa, I., Aokage, T., Nishimaki, K., Matsumoto, K., Takahashi, H., Asoh, S., Teramoto, A., and Ohta, S. (2005) *J. Neurooncol.* **72,** 231–238
36. Fulda, S., Wick, W., Weller, M., and Debatin, K. M. (2002) *Nat. Med.* **8,** 808–815
37. Schimmer, A. D., Welsh, K., Pinilla, C., Wang, Z., Krajewska, M., Bonneau, M. J., Pedersen, I. M., Kitada, S., Scott, F. L., Bailly-Maitre, B., Glinsky, G., Scudiero, D., Sausville, E., Salvesen, G., Nefzi, A., Ostresh, J. M., Houghten, R. A., and Reed, J. C. (2004) *Cancer Cell* **5,** 25–35
38. Wang, J. F., and Hill, D. J. (2009) *J. Endocrinol.* **201,** 15–25
39. Lee, Y., Scheck, A. C., Cloughesy, T. F., Lai, A., Dong, J., Farooqi, H. K., Liau, L. M., Horvath, S., Mischel, P. S., and Nelson, S. F. (2008) *BMC Medical Genomics* **1,** 52–63
40. Kim, Y. J., Yoon, S. Y., Kim, J. T., Song, E. Y., Lee, H. G., Son, H. J., Kim, S. Y., Cho, D., Choi, I., Kim, J. H., and Kim, J. W. (2009) *Carcinogenesis* **30,** 598–605
41. Lorentzen, A., Vogel, L. K., Lewinsky, R. H., Saebø, M., Skjelbred, C. F., Godiksen, S., Hoff, G., Tveit, K. M., Lothe, I. M., Ikdahl, T., Kure, E. H., and Mitchelmore, C. (2007) *BMC Cancer* **7,** 192–199
42. Zhao, H., Zhang, J., Lu, J., He, X., Chen, C., Li, X., Gong, L., Bao, G., Fu, Q., Chen, S., Lin, W., Shi, H., Ma, J., Liu, X., Ma, Q., and Yao, L. (2008) *BMC Cancer* **8,** 303–311
43. Lee, D. C., Kang, Y. K., Kim, W. H., Jang, Y. J., Kim, D. J., Park, I. Y., Sohn, B. H., Sohn, H. A., Lee, H. G., Lim, J. S., Kim, J. W., Song, E. Y., Kim, D. M., Lee, M. N., Oh, G. T., Kim, S. J., Park, K. C., Yoo, H. S., Choi, J. Y., and Yeom, Y. I. (2008) *Cancer Res.* **68,** 4210–4220
44. Choi, S. C., Yoon, S. R., Park, Y. P., Song, E. Y., Kim, J. W., Kim, W. H., Yang, Y., Lim, J. S., and Lee, H. G. (2007) *Exp. Mol. Med.* **39,** 705–714
45. Ma, J., Jin, H., Wang, H., Yuan, J., Bao, T., Jiang, X., Zhang, W., Zhao, H., and Yao, L. (2008) *Biol. Pharm. Bull* **31,** 1316–1320
46. Kim, Y. J., Yoon, S. Y., Kim, J. T., Choi, S. C., Lim, J. S., Kim, J. H., Song, E. Y., Lee, H. G., Choi, I., and Kim, J. W. (2009) *Int. J. Cancer* **124,** 7–15
47. Liu, N., Wang, L., Li, X., Yang, Q., Liu, X., Zhang, J., Zhang, J., Wu, Y., Ji, S., Zhang, Y., Yang, A., Han, H., and Yao, L. (2008) *Nucleic Acids Res.* **36,** 5335–5349
48. Angst, E., Sibold, S., Tiffon, C., Weimann, R., Gloor, B., Candinas, D., and Stroka, D. (2006) *Br. J. Cancer* **95,** 307–313
49. Bandyopadhyay, S., Pai, S. K., Gross, S. C., Hirota, S., Hosobe, S., Miura, K., Saito, K., Commes, T., Hayashi, S., Watabe, M., and Watabe, K. (2003) *Cancer Res.* **63,** 1731–1736
50. Dang, C., Gottschling, M., Manning, K., O'Currain, E., Schneider, S., Sterry, W., Stockfleth, E., and Nindl, I. (2006) *Oncol. Rep.* **16,** 513–519
51. Fotovati, A., Fujii, T., Yamaguchi, M., Kage, M., Shirouzu, K., Oie, S., Basaki, Y., Ono, M., Yamana, H., and Kuwano, M. (2006) *Clin. Cancer Res.* **12,** 3010–3018
52. Shah, M. A., Kemeny, N., Hummer, A., Drobnjak, M., Motwani, M., Cordon-Cardo, C., Gonen, M., and Schwartz, G. K. (2005) *Clin. Cancer Res.* **11,** 3296–3302
53. Kurdistani, S. K., Arizti, P., Reimer, C. L., Sugrue, M. M., Aaronson, S. A., and Lee, S. W. (1998) *Cancer Res.* **58,** 4439–4444
54. Stein, S., Thomas, E. K., Herzog, B., Westfall, M. D., Rocheleau, J. V., Jackson, R. S., 2nd, Wang, M., and Liang, P. (2004) *J. Biol. Chem.* **279,** 48930–48940
55. Bandyopadhyay, S., Pai, S. K., Hirota, S., Hosobe, S., Tsukada, T., Miura, K., Takano, Y., Saito, K., Commes, T., Piquemal, D., Watabe, M., Gross, S., Wang, Y., Huggenvik, J., and Watabe, K. (2004) *Cancer Res.* **64,** 7655–7660
56. Wang, W., Li, Y., Li, Y., Hong, A., Wang, J., Lin, B., and Li, R. (2009) *Int. J. Cancer* **124,** 521–530
57. Kovacevic, Z., and Richardson, D. R. (2006) *Carcinogenesis* **27,** 2355–2366
58. Yao, L., Zhang, J., and Liu, X. (2008) *Acta Biochim. Biophys. Sin (Shanghai)* **40,** 625–635